Chemistry & Biology, Vol. 10, 939–952, October, 2003, ©2003 Elsevier Science Ltd. All rights reserved. DOI 10.1016/j.chembiol.2003.09.012

Melithiazol Biosynthesis: Further Insights into Myxobacterial PKS/NRPS Systems and Evidence for a New Subclass of Methyl Transferases

Stefan Weinig,[1,2] Hans-Jürgen Hecht,[1] Taifo Mahmud,[3] and Rolf Müller[1,2,*]

[1]Gesellschaft für Biotechnologische Forschung mbH (GBF)
Mascheroder Weg 1
38124 Braunschweig
[2]Institut für Pharmazeutische Biologie
Mendelssohnstr. 1
Technische Universität
38106 Braunschweig
Germany
[3]University of Washington
Department of Chemistry
Seattle, Washington 98195

Summary

A DNA region of 41.847 base pairs from *Melittangium lichenicola* Me I46 is shown to be responsible for the biosynthesis of the potent electron transport inhibitor melithiazol. Melithiazol is formed by a combined polyketide synthase/peptide synthetase system resembling the myxothiazol megasynthetase from *Stigmatella aurantiaca* DW4/3-1. Both natural products share an almost identical core region but employ different starter molecules. Additionally, melithiazol contains a terminal methyl ester instead of the amide moiety found in myxothiazol. Similar to myxothiazol formation, the methyl ester is formed via an amide intermediate, which is converted by a hydrolase and an unusual type of SAM (S-adenosyl-L-methionine)-dependent methyltransferase into the methyl ester. When transferred into the myxothiazol A (amide) producer, these two genes lead to the formation of the methyl ester of myxothiazol. The methyl transferase described is a member of a protein subfamily of a previously unknown function lacking a typical SAM binding motif.

Introduction

Polyketide synthases (PKSs) and nonribosomal peptide synthetases (NRPSs) are important enzymatic systems which are responsible for the formation of an immense variety of natural products [1–3]. Starting from simple building blocks, such as short chain carboxylic acids and amino acids, secondary metabolites with various biological activities are assembled in microorganisms. The resulting low molecular weight polyketides and polypeptides are widely used by the pharmaceutical and agrochemical industry (e.g., erythromycin, rapamycin, FK506, cyclosporin, avermectin, lovastatin, and epothilone).

Both PKSs and NRPSs are characterized as large, multifunctional, and modular enzyme complexes which assemble secondary metabolites in a stepwise fashion. Their corresponding biosynthetic machineries are interesting targets for genetic engineering and mutasynthesis strategies aimed at the production of novel and altered structures, ideally giving rise to substances with improved biological activities. The monomers used are coenzyme A esters of short chain carboxylic acids in PKSs and amino acids in NRPSs. These precursors are attached as thioesters to carrier proteins via a phosphopantetheinyl arm that needs to be transferred posttranslationally to conserved serine residues in each carrier protein [4]. The selection for each monomer is performed by acyl transferase domains (AT domains in PKS) and adenylation domains (A domains in NRPS). After loading of the megasynthetase, the condensation reactions between the monomers are catalyzed by ketosynthase (KS) domains in PKS and by condensation (C) domains in NRPS, which leads to the formation of carbon-carbon bonds by Claisen ester condensation and to peptide linkages, respectively.

During the last few years, hybrid systems employing PKS and NRPS biochemistry in the course of the assembly of one product have been reported [5–7], which resulted in intensified studies aimed at the combination of PKS/NRPS assembly lines for combinatorial biosynthesis [8–10].

Although relatively rarely studied in comparison to actinomycetes, myxobacteria have been shown to be a major source of secondary metabolites, especially those that show the typical features of PKS/NRPS hybrids: the incorporation of amino acids and short chain carboxylic acids into their backbones [11]. Cloning of the responsible genes revealed biosynthetic enzymes that harbor PKS and NRPS modules, even present on one single open reading frame [12, 13], and a variety of other novel features have been described from multimodular myxobacterial systems [14–19]. Cyanobacteria seem to be equally rich in "nonstandard" biosynthetic systems, as has been shown in recent genetic studies [20–22].

Myxothiazol [23, 24] and melithiazol [25, 26] represent two highly efficient electron transport inhibitors of the eukaryotic respiratory chain which are produced by the myxobacteria *Stigmatella aurantiaca* DW4/3-1 and *Melittangium lichenicola* Me I46, respectively. These compounds are similar, but some significant biosynthetic differences can be expected due to structural differences (see Figure 1). The myxothiazol hybrid PKS/NRPS biosynthetic gene cluster was analyzed mainly based on in silico analysis of the corresponding biosynthetic genes [12].

In order to explore the structural diversity and the underlying biosynthetic mechanisms as well as the evolutionary origin of the biosynthetic machineries, we cloned and analyzed the melithiazol gene cluster. Biosynthetic origins of the unusual isobutyrate starter unit and the terminal methyl ester in melithiazol as well as the terminal amide in myxothiazol were analyzed using classical feeding experiments. Additionally, by heterologous expression a novel type of SAM-dependent methyl transferase and a hydrolase are shown to be involved

*Correspondence: rom@gbf.de

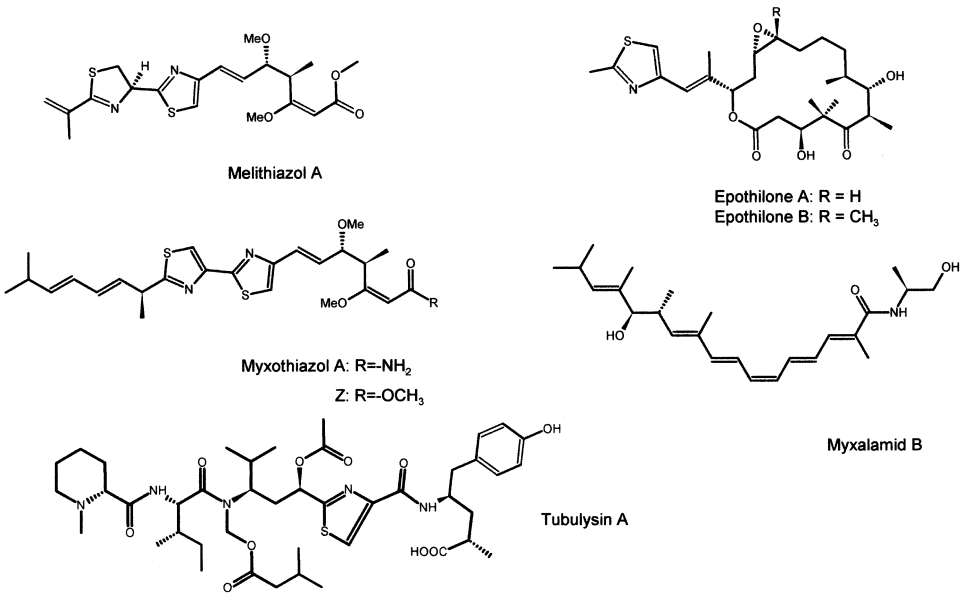

Figure 1. Examples for Myxobacterial Secondary Metabolites which Are Biosynthesized by PKS and NRPS

in the methyl ester formation starting from an amide intermediate.

Results and Discussion

Cloning and Analysis of the Melithiazol Biosynthetic Gene Cluster

Due to the structural similarity of myxothiazol and melithiazol, the genes involved in their biosynthesis were expected to be similar in sequence. In Southern blot experiments, it could be shown that genomic DNA of *M. lichenicola* Me I46 hybridized under stringent conditions with *mtaE* and *mtaF* gene probes. A cosmid library of *M. lichenicola* Me I46 was prepared and used for colony hybridzation experiments, resulting in the identification of a cosmid (M1) that gave positive signals with both probes. End sequences from cosmid M1 (T3 and the T7 ends) were compared to the myxothiazol gene cluster, revealing M1 to harbor a fragment of the melithiazol gene cluster starting with the AT domain of the *mtaE* analog *melE* (see Figure 2A). Using oligonucleotides designed to bind to this end sequence, cosmid pools of the gene library were screened for the presence of overlapping cosmids [12]. These were subjected to end sequencing, and the derived sequences were used to locate the rest of the melithiazol gene cluster on cosmid M2 (M2 ends in the AT of the *mtaF* analog *melF*). Cosmids M1 and M2 were sequenced and revealed the presence of several open reading frames (ORFs) with similarity to PKSs and NRPS, which were designated *melB-K* (*mel*ithiazol; see Figure 2A). No gene encoding a phosphopantetheinyl (Ppant)-transferase similar to *mtaA* was found. MtaA was shown to have a broad substrate specificity [27] and is required for the production of myxothiazol [12] and at least two additional PKS and PKS/NRPS hybrid compounds produced by *S. aurantiaca* DW4/3-1 (G. Höfle, S. Wenzel, H. Bode, and R.M., unpublished data; [28]). It is thus likely that similar to *S. aurantiaca* DW4/3-1, *M. lichenicola* Me I46 uses only one secondary metabolic Ppant transferase, which must be encoded outside of the melithiazol biosynthetic gene cluster.

Analysis of the modular structure of the melithiazol megasynthetase revealed that *melB* most likely encodes the first module of the biosynthetic gene cluster (see below). The modular organization of PKSs and NRPSs involves activation and condensation of the following carboxylic acid or amino acid onto the growing chain catalyzed by an acyl-transferase (AT) domain and a KS domain (PKS) or an adenylation (A) and a condensation (C) domain (NRPS). The resulting β-keto acid (oligopeptide in NRPS) may subsequently be processed by β-keto-acyl-reductase (KR) domains, β-hydroxy-acyl-dehydratase (DH) domains, and enoyl-reductase (ER) domains or N-methyl transferase (N-MT) and epimerase (E) domains in NRPS (reviewed in [1]). Additional domains for C-methylation [29, 30] and O-methylation [12, 18] of intermediates have recently been reported, and the function of heterocyclization (HC) and oxidation (Ox) domains involved in the formation of oxazoline and thiazoline rings and their subsequent oxidation to oxazole and thiazole structures has been elucidated [3, 31, 32].

Sequence motifs typical for PKS domains [33, 34] and NRPS domains [3, 35] were detected in MelB-G (Table 1 and Figure 2B). The acyl carrier protein domains (ACP) and the peptidyl carrier protein (PCP) domain of MelB-G contain the Prosite consensus signature of the putative binding site for the 4′-phosphopantetheine (Ppant) cofactor (Prosite signature numbers PS00012, R2082, and L2104). The codon bias of the genes reported is in accordance with other genes from myxobacteria [36]. The overall G+C content of the *mel*-biosynthetic gene cluster, which spans approximately 42 kbp, is 69.7%.

Eight further ORFs were identified upstream and downstream of the melithiazol PKS/NRPS genes. Based on the sequence similarities of the encoded proteins to

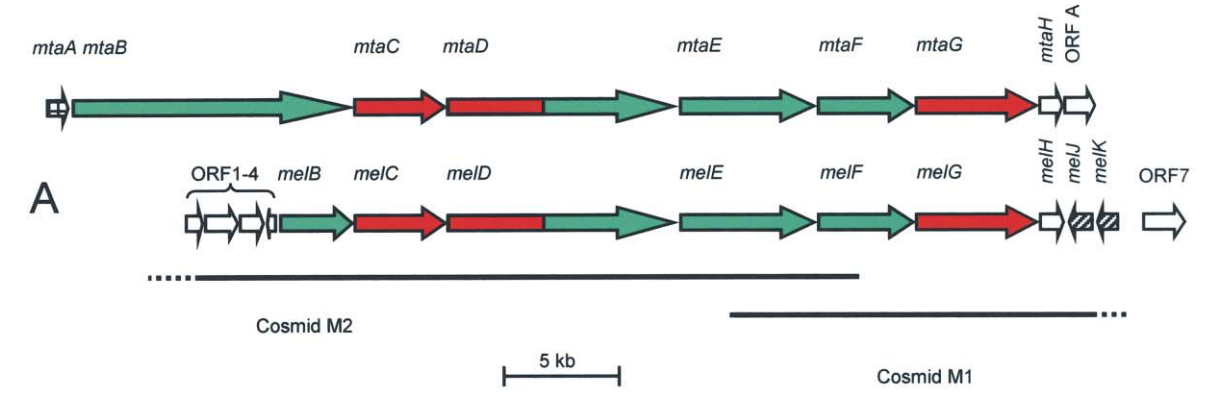

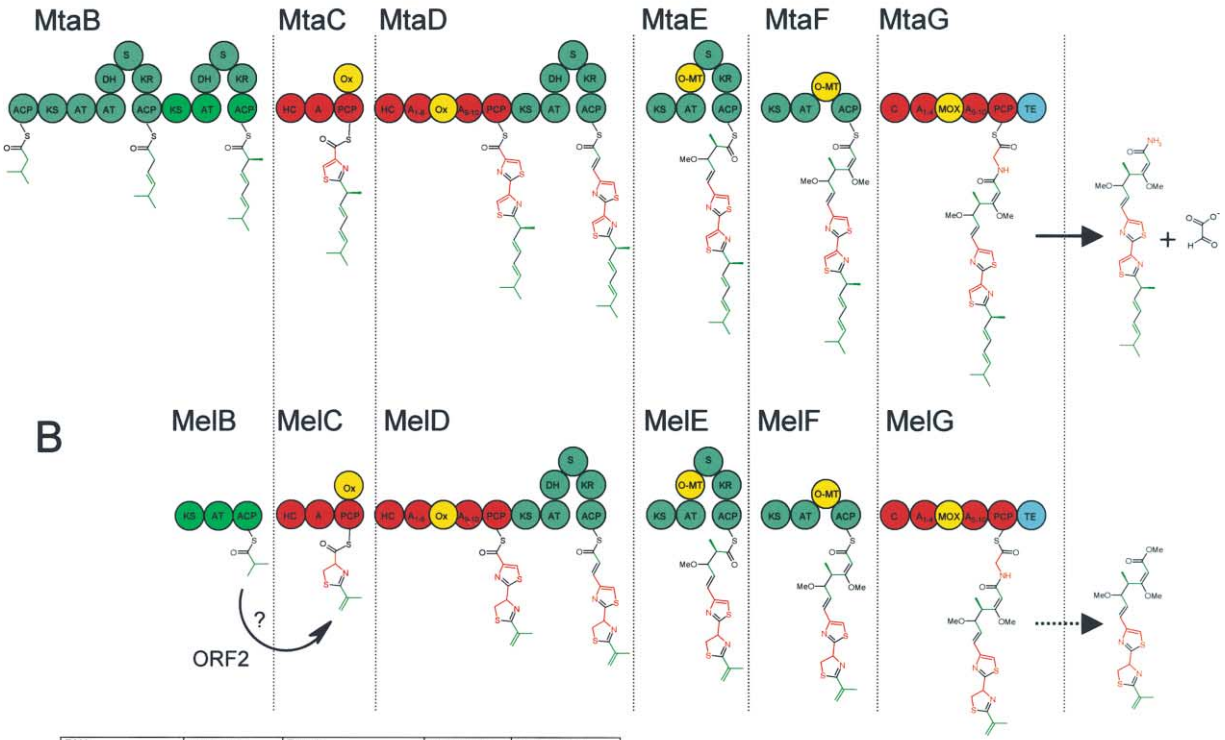

DNA	Identity [%]	Protein	Identity [%]	Similarity [%]
melB / mtaB		MelB / MtaB		
KS-AT / KS_2-AT_3	73	KS-AT / KS_2-AT_3	67	78
ACP / ACP_3	72	ACP / ACP_3	64	78
melC / mtaC	71	MelC / MtaC	63	76
melD / mtaD	72	MelD / MtaD	60	72
melE / mtaE	75	MelE / MtaE	66	76
melF / mtaF	77	MelF / MtaF	69	82
melG / mtaG	75	MelG / MtaG	72	83
melH / mtaH	79	MelH / MtaH	72	85

Figure 2. The *mta* and *mel* Biosynthetic Gene Clusters

(A) Comparison of gene arrangements in the *mta* and *mel* biosynthetic gene clusters. Arrows indicate the direction of transcription of each gene. The checkered arrow symbolizes *mtaA* encoding a phosphopantetheinyl transferase. PKS modules are shown in green, NRPS modules are shown in red, and ORFs with unknown function are depicted in white. Hatched arrows indicate genes encoding modifying enzymes. PKS, polyketide synthase; NRPS, nonribosomal peptide synthetase.

(B) Models of myxothiazol and melithiazol biosynthesis. PKS modules are colored in green, NRPS modules are shown in red, and unusual domains are shown in yellow. Domains depicted in light green are assumed to be derived from each other (see text). The TE domain is shown in blue. Building blocks incorporated by PKS modules are depicted with green bonds, whereas molecule moieties assembled by NRPS modules are shown with red bonds. ACP, acyl carrier protein; KS, β-ketoacyl-ACP synthase; KR, β-ketoacyl-ACP reductase; AT, acyl transferase; DH, β-hydroxy-acyl-ACP dehydratase; O-MT, O-methyl transferase; ER, enoyl reduktase; S, spacer region; PCP, peptidyl carrier protein; C, condensation domain; HC, heterocyclization domain; A, adenylation domain; Ox, oxidation domain; MOX, monooxygenase domain; TE, thioesterase.

Table 1. Deduced Functions of ORFs in the Melithiazol Biosynthetic Gene Cluster

A. PKS and NRPS Parts of the Gene Cluster

Protein (Gene)	Size (bp/Da)	Proposed Function (Protein Domains with Their Position in the Sequence)
MelB (*melB*)	3,153 bp, 111,621 Da	PKS domains: KS (16-443), AT (555-870), ACP (962-1028)
MelC (*melC*)	3,972 bp, 146,206 Da	NRPS domains: HC (52-452), A (538-1001), PCP (1025-1093) Ox (1025-1093)
MelD (*melD*)	9,855 bp, 357,430 Da	NRPS domains: HC (74-473), A (560-1291), Ox (989-1241), PCP (1319-1383); PKS domains: KS (1447-1874), AT (1981-2296), DH (2307-2521), S (2612-2849), KR (2882-3134), ACP (3157-3226)
MelE (*melE*)	5,739 bp, 206,932 Da	PKS domains: KS (35-429), AT (573-890), O-MT (972-1246), S (1252-1454), KR (1486-1746), ACP (1783-1849)
MelF (*melF*)	4,083 bp, 148,434 Da	PKS domains: KS (39-464), AT (571-886), O-MT (946-1221), ACP (1272-1338)
MelG (*melG*)	5,247 bp, 192,469 Da	NRPS domains: C (68-367), A (555-1380), MonoOx (753-1114), PCP (1401-1469), TE (1488-1748)

B. ORFs Encoded Upstream and Downstream of *melB-melG*

Protein (Gene)	Size (bp/Da)	Proposed Function of the Similar Protein	Sequence Similarity to (Source Plus Additional Available Information)	Similarity/Identity	Accession No. of the Similar Protein
ORF1 (*orf1*)	699 bp, 24,529 Da	Similar to glycosyl transferases	*Archaeoglobus fulgidus*	40%/28%	C69298
ORF2 (*orf2*)	1,359 bp, 48,004 Da	L-amino acid oxidase	*Crotalus adamanteus*	70%/51%	JE0266
ORF3 (*orf3*)	963 bp, 35,377 Da	Nucleotide sugar epimerase	*Escherichia coli* WbnF	64%/48%	AAD50494
ORF4 (*orf4*)	282 bp, 10,290 Da	Glutaredoxin	*Yersinia pestis* GrxC	59%/45%	NP_403730
MelH (*melH*)	990 bp, 36,189 Da	2-hydroxyhepta-2,4-diene-1,7-dioate-isomerase	*Methanothermobacter thermautotrophicus* MTH1507	56%/40%	A69068
MelJ (*melJ*)	1,088 bp, 37,051 Da	Nitrilase	*Arabidopsis thaliana* NIT3	39%/26%	P46010
MelK (*melK*)	906 bp, 33,612 bp	Methyl transferase	*Actinosynnema pretiosum* Asm10	41%/28%	AF453501.1
ORF7 (*orf7*)	1,788 bp 64,332 Da	ABC-transporter	*Nostoc punctiforme* Npun4209	61%/44%	ZP_00109759

proteins from the databases, ORF2, MelJ, and MelK seemed to be involved in the biosynthesis of melithiazol (see Table 1 and Figures 2A and 4). The gene encoding MelH is located directly behind *melG*, which is similar to the gene order in the *mta* gene cluster. Nevertheless, *melH* and *mtaH* do not seem to be required for melithiazol and myxothiazol biosynthesis (see the accompanying manuscript [65] for a discussion of the putative function of *melH*).

Model for the Melithiazol Biosynthetic Pathway

Here it is demonstrated that the melithiazol biosynthetic machinery is very similar to the myxothiazol system and belongs to the class of hybrid biosynthetic systems composed of PKS and NRPS modules. The biosynthesis switches from PKS type biochemistry (MelB) to NRPS (MelCD), back to PKS (MelDEF), and finally back to NRPS (MelG). MelD belongs to the few known proteins in which a NRPS module is covalently linked to a PKS module, which makes it an ideal target to study PKS/NRPS interaction.

The modular structure of type I PKSs usually starts with an AT or a CoA-ligase domain responsible for the recognition (and, in the case of CoA-ligases, for activation) of the starter molecule followed by transfer of the activated substrate to the first ACP domain (compare the biosynthetic gene clusters of erythromycin [33], rapamycin [5, 34], and rifamycin [6]). Alternative starters can be used to initiate the biosynthesis of the polyketides, but most frequently acetyl-CoA, malonyl-CoA, propionyl-CoA, or methylmalonyl-CoA are employed. If activated dicarboxylic acids are used, modified KS domains can be found at the beginning of the first module. These have lost their condensation activity but effectively decarboxylate the ACP-bound dicarboxylic acid, giving rise to the starter moiety. Because the active site cysteine of these KS domains is mutated to glutamine, they have been designated KS_Q domains [37]. In the case of *melB*, the modular organization looks similar: the protein starts with a KS domain that is followed by an AT and an ACP domain.

Several myxobacterial PKSs show an atypically arranged starter module with ACP-KS-AT-AT-KR-ACP [12, 18, 19, 38]. In these systems the first AT loads the starter molecule, whereas the second AT loads the first extender unit ([39]; P. Leadlay, C. Wilkinson, S.W., and R.M., unpublished data). *M. lichenicola* Me l46 produces only melithiazol A (and melithiazol C, which is presumably a degradation product), which is characterized by a dehydro-isobutyrate starter molecule [26]. Myxobac-

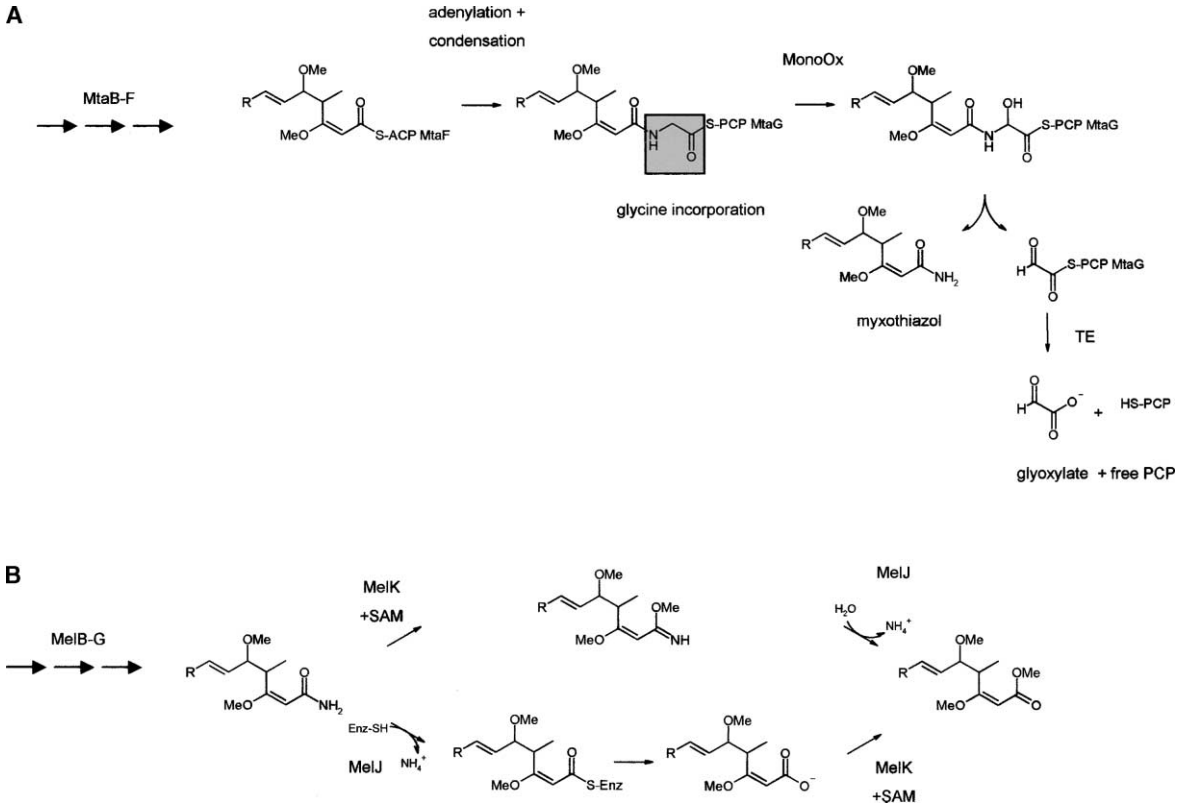

Figure 3. Models for Amide and Methyl-Ester Formation

(A) Model of terminal amide formation. The glycine used for the extension of myxothiazol acid by MtaG is shown shaded. See text and [12].
(B) Model of methyl-ester formation starting from the amide. The upper route via the imino-ester has been postulated recently [50]. Alternatively, MelJ might hydrolyze the amide, and MelK could next methylate the free acid (see text).

teria frequently employ activated short branched chain carboxylic acids as starter molecules for PKS, e.g., isobutyrate and 2-methyl-butyrate in myxalamid and isovalerate in myxothiazol biosynthesis [12, 19, 40]. Although these starter molecules are generally thought to be derived from branched chain amino acids by amino acid degradation, it has recently become clear that in myxobacteria a novel branch of the mevalonate pathway is used as an alternative source of at least isovalerate [41]. We expected the dehydro-isobutyrate starter of melithiazol to be derived from valine degradation and subsequent oxidation. In order to verify this hypothesis, d8-DL-valine was fed to the culture broth, and incorporation rates of approximately 50% were detected using LC-MS analysis (melithiazol, $M + H^+ = 423$; d5-melithiazol, $M + H^+ = 428$; data not shown).

The active site cysteine is present in position 189 of the MelB-KS, which indicates that it does not represent a KS_Q domain. In addition, AT domains located in KS_Q-containing modules load dicarboxylic acids onto the PKS. They are known to contain a highly conserved arginine residue [42] that is replaced by a serine in the MelB-AT. It is thus likely that the MelB-AT domain loads isobutyryl-CoA onto the ACP. Because there is no indication from the primary sequence that the MelB-KS is inactive, the function of this domain remains obscure. It is not clear at which stage of the biosynthesis the oxidation of the isopropyl moiety occurs; ORF2 is the protein most likely involved, because it resembles amino acid oxidases (see Table 1). The oxidation might take place at any step between the amino acid and the ACP-bound isobutyrate.

Next, MelC activates cysteine (see Supplemental Table S1 at http://www.chembiol.com/cgi/content/full/10/10/939/DC1; the A domain perfectly matches the nonribosomal code [43, 44]), performs the first heterocyclization, and transfers the thiazoline-intermediate to MelD. Interestingly, MelC contains an Ox domain located behind the PCP, which is similar to the structure of MtaC. Nevertheless, *M. lichenicola* Me I46 is only known to produce thiazoline-thiazole type melithiazols, which raises the question of the function of this Ox domain in both biosynthetic systems. The deletion of the MtaC-Ox domain leads to a producer of unchanged myxothiazol. Thus, it seems likely that the Ox domains of MtaC and MelC are superfluous or inactive per se (see accompanying manuscript [65]). MelD is similar to MtaD and harbors two modules: one NRPS module with another Ox domain that is inserted between the core motifs of A domains A8 and A9 instead of being localized behind the PCP in MelC. The thiazoline-thiazole intermediate is then transferred to the PKS module of MelD, which extends with malonate and reduces and dehydrates the β-keto-thioester to its enoyl-form. Large spacer regions (S) are located between the DH and the KR domains of the PKS module of MelD and between the O-MT and

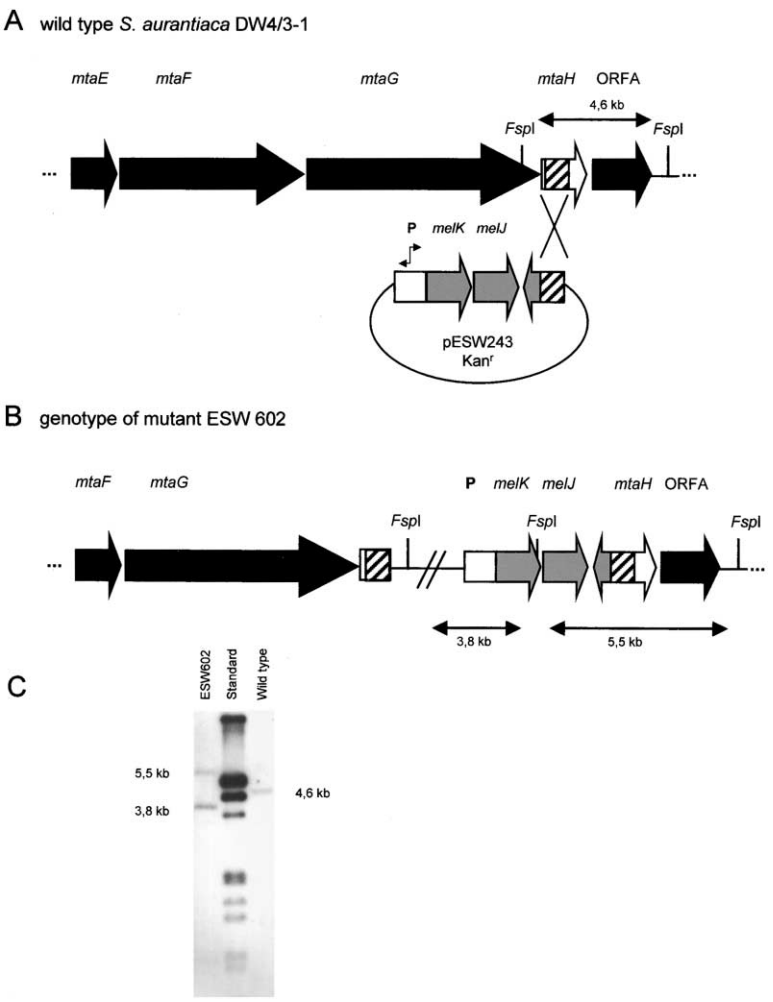

Figure 4. Heterologous Expression of MelK and MelJ

(A) Schematic diagram showing the chromosomal integration of *melJK* from *M. lichenicola* Me I46 into *S. aurantiaca* DW4/3-1. Genes are shown as arrows, and the homologous region from *mtaH* used for integration is hatched (this DNA fragment encodes part of *mtaH* and is oriented in the opposite direction to the rest of the *melH* gene encoded by pESW243). P indicates the presumed bidirectional promoter regulating the transcription of *melJK*. FspI shows the position of the recognition sequence of the respective restriction enzyme.

(B) Genotype of the merodiploid strain ESW602 resulting from integration of pESW243 into the chromosome of *S. aurantiaca* DW4/3-1.

(C) Southern blot analysis of ESW602 and *S. aurantiaca* DW4/3-1 after restriction with FspI. A DNA fragment containing the promoter region of *melJK, melJK*, and *melH* was used as a probe (3.2 kb). The size of the hybridizing fragments was estimated using DIG-labeled DNA molecular weight marker III (Roche Diagnostics). Hybridizing fragments and their sizes are indicated in (A) and (B). *S. aurantiaca* DW4/3-1 chromosomal DNA shows a signal because *mtaH* and *melH* are very similar on the DNA level (78.6% identity over 680 bp).

KR domains of MelE. These have been described for almost all PKS and fatty acid biosynthetic systems [1, 45], but their function is not clear. S regions can also be found in all myxobacterial PKS systems sequenced so far and show an identity of up to 35% on the amino acid level.

MelE is another peculiar enzyme; between the AT domain and the spacer region an O-MT domain can be found that has only been reported in two other biosynthetic systems, both from myxobacteria [12, 18]. This domain is assumed to methylate the intermediate after ketoreduction, giving rise to the methyl ether. The O-MT domain of MelE is similar to O-MT domains of MelF, MtaE, MtaF, StiD, and StiE and shows the typical primary amino acid sequences involved in SAM binding [46] (see Supplemental Figure S1A at *Chemistry & Biology*'s website). Feeding experiments employing ^{13}C-labeled methionine were performed, the results of which prove that both O-MT domains employ SAM as cofactor (incorporation rates for the three SAM-derived methyl groups in melithiazol were between 16% and 21%, see below). The methylmalonate extended intermediate is transferred to MelF, which activates malonate. Again, similar biochemistry is performed in comparison to the unique myxothiazol system: an O-MT domain gives rise to the methylation of the enol form of the β-keto intermediate bound to the ACP. Interestingly, the O-MT sequences of MelF and MtaF show more identity than those of MelE and MelF (see Supplemental Figure S1B), which suggests that they are specialized for different biochemical reactions.

Unexpectedly, MelG, a MtaG homolog, was found at the end of the PKS/NRPS part of the gene cluster. MtaG is believed to be involved in the formation of the terminal amide of myxothiazol (see below). Thus, we expected to find some genes responsible for methyl ester formation, starting from the thioesterified myxothiazol acid bound to the ACP of MelF. Due to the fact that MelG closely resembles MtaG, we concluded that melithiazol is formed via the amide form of the melithiazol acid. The unusual mechanism of amide formation by MtaG/MelG is discussed in the next paragraph.

Establishing the Biosynthetic Precursors of the Terminal Methyl Ester and Amide Functionalities by Feeding Experiments

The terminal gene of the myxothiazol gene cluster (*mtaG*) resembles an unusual NRPS with an integrated monooxygenase (MonoOx) domain, which led us to suggest that MtaG is involved in the formation of the terminal amide

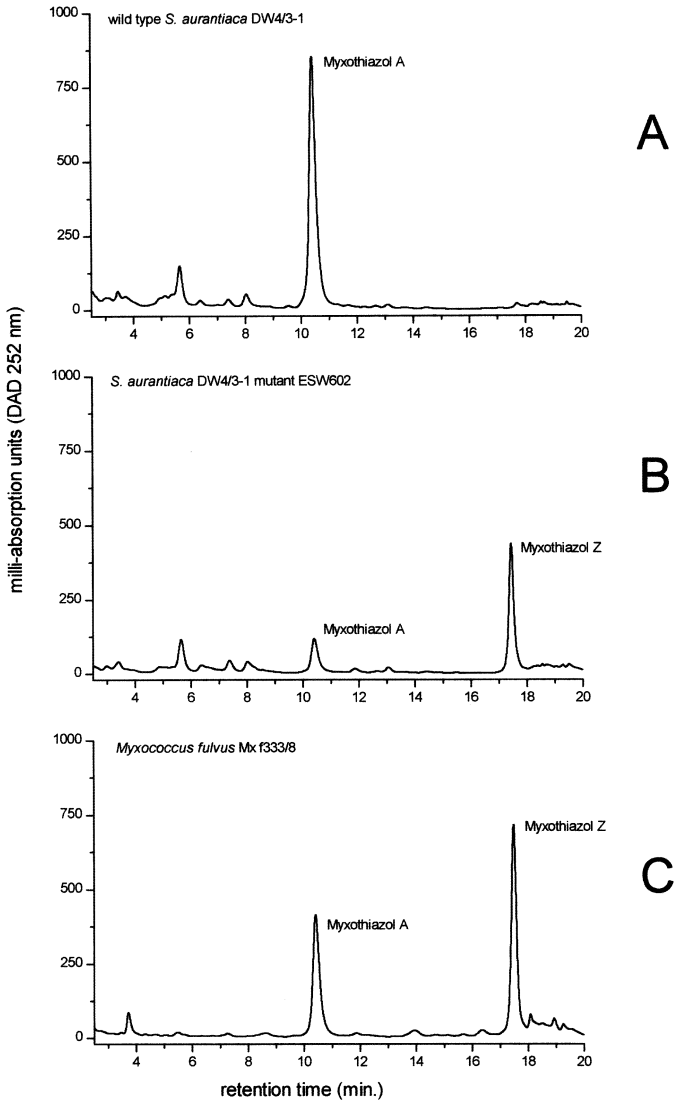

Figure 5. Production of Secondary Metabolites in *S. aurantiaca* DW4/3-1, Mutant ESW602, and *M. fulvus* Mx f333/8

HPLC analysis of the extracts from *S. aurantiaca* DW4/3-1 (A), mutant ESW602 (B), and the myxothiazol A and Z producer *M. fulvus* Mx f333/8 (C).

via the addition of an extra amino acid to the MtaF-ACP-bound myxothiazol acid. Subsequently, the carbon backbone of this amino acid is removed by the action of the MtaG MonoOx domain, resulting in the terminal amide structure (see Figure 3; [12]).

Terminal amides are found in many bioactive substances from mammals and insects, including many peptide hormones [47, 48]. Generally, they arise from the oxidative cleavage of C-terminal glycine-extended precursors by a bifunctional copper-zinc-dependent enzyme, peptidylglycine α-amidating monooxygenase [47, 48]. The process requires two reaction steps. The first involves ascorbate- and copper-dependent aerobic hydroxylation of the glycine α-carbon by peptidylglycine α-hydroxylating monooxygenase. The second step, the cleavage of the resulting carbinolamide, is catalyzed by a zinc-dependent enzyme, peptidylamidoglycolate lyase. We assumed that the MtaG MonoOx domain would perform a similar reaction and hydroxylate the amino acid-extended myxothiazol in the α position, which should result in an intermediate that can fall apart spontaneously (or catalyzed by MtaG), giving rise to myxothiazol and glyoxylic acid thioesterified to the PCP of MtaG. The thioesterase at the C terminus of MtaG would thus be needed to release the glyoxylate from the PCP to deblock the enzyme.

To strengthen this hypothesis, we tried to identify the nitrogen source of the terminal amide of myxothiazol in a series of incorporation experiments. The putative donor amino acids were chosen after analysis of the MtaG region responsible for the specificity of A domains for their putative binding pocket [43, 44], which is rather difficult in MtaG (and MelG as well) due to the insertion of the MonoOx domain next to the binding pocket. Nevertheless, both amino acid regions were indicative of glycine as the amino acid used (see Supplemental Table S1 at *Chemistry & Biology*'s website). We therefore reasoned that feeding of ^{15}N-labeled glycine should result in incorporation of the label into myxothiazol. Indeed, using mass spectrometry of isolated myxothiazol, the result of the feeding experiment showed 40.6% incorporation of ^{15}N-glycine into the compound (data not shown),

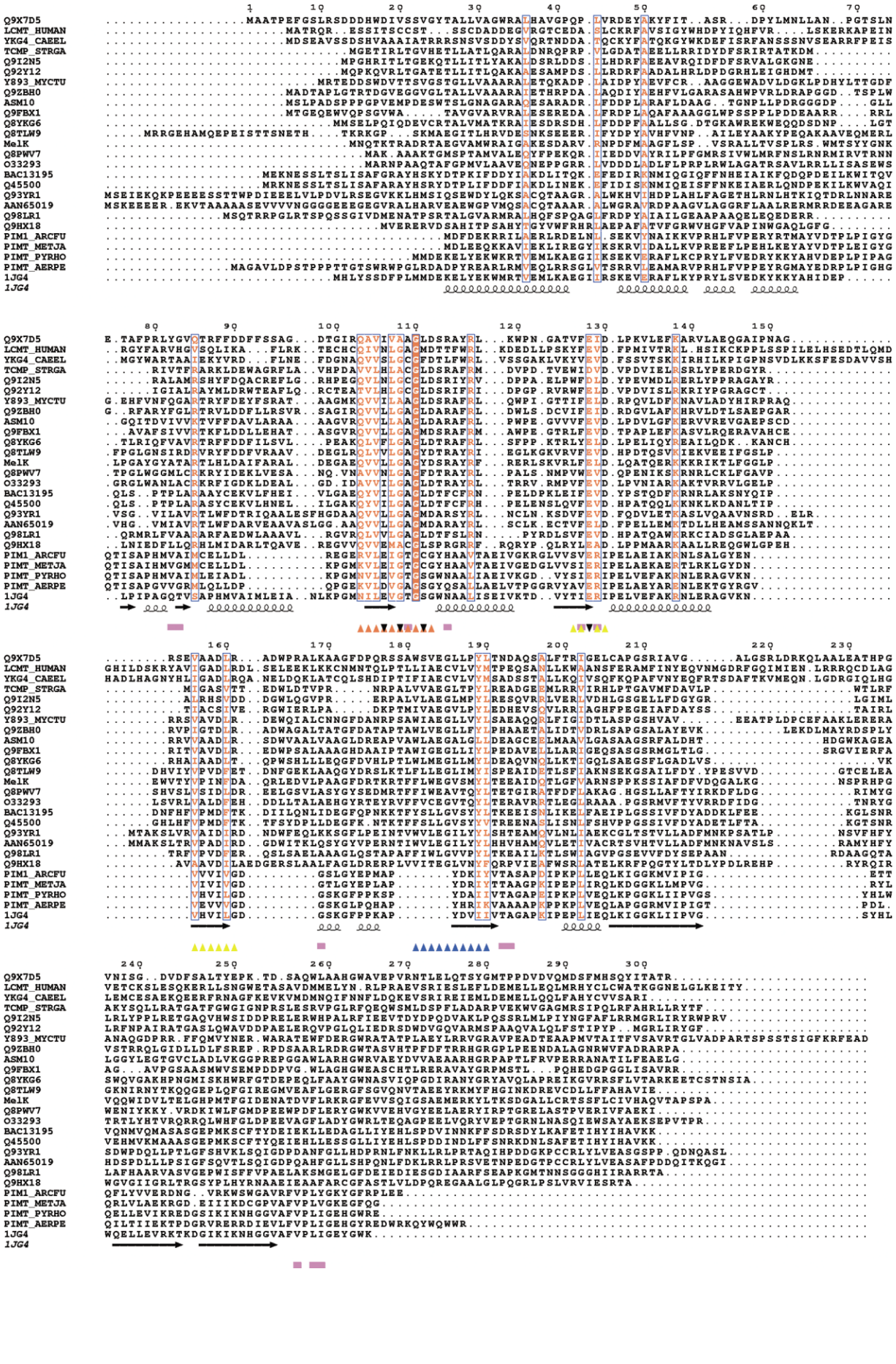
Q9X7D5
LCMT_HUMAN
YKG4_CAEEL
TCMP_STRGA
Q9I2N5
Q92Y12
Y893_MYCTU
Q9ZBH0
ASM10
Q9FBX1
Q8YKG6
Q8TLW9
MelK
Q8PWV7
O33293
BAC13195
Q45500
Q93YR1
AAN65019
Q98LR1
Q9HX18
PIM1_ARCFU
PIMT_METJA
PIMT_PYRHO
PIMT_AERPE
1JG4
1JG4

whereas ^{15}N-labeled glutamate and ammonium chloride were not incorporated at all. This suggests that the terminal amide of myxothiazol is derived directly from an extra glycine that is intermediary attached to the molecule. Interestingly, serine has been shown to be the nitrogen source of the terminal amide of nosiheptide [49], which indicates a similar mechanism for amide formation in the producer *Streptomyces actuosus* and possibly for other natural products with terminal amide moieties as well (e.g., thiostreptone).

Currently, two more examples of NRPS with inserted MonoOx domains can be found in the databases (hypothetical proteins from *Nostoc punctiforme* and *Ralstonia solanacearum* which show the domain structure A-MonoOx-PCP-KS-AT-ACP-Aminotransferase-C-A-PCP... and ...KS-AT-ACP-Aminotransferase-MonoOx-C-A-PCP..., respectively). None of these proteins seems to be involved in terminal amide formation, because the MonoOx domains are not within the C-terminal modules, nor are they located within an A domain. Nevertheless, both proteins belong to the class of PKS/NRPS hybrids. In contrast, the unusual arrangement of domains in MtaG can be found in MelG as well (see Figure 2B). It is thus reasoned that melithiazol in close biosynthetic analogy is also formed via the amide intermediate. This would represent a unique mechanism to generate a methyl ester, because the glycine extender has to be removed completely in order to generate the ester. It seemed likely that melithiazol is biosynthesized by a methyl transferase (which would presumably employ SAM as cofactor) and a hydrolase. The gene products of *melK* and *melJ*, which are located downstream of *melG*, indeed show some similarities to such enzymes (Table 1). To verify the dependence of the methyl ester formation on a SAM-dependent enzyme, a feeding experiment employing [$^{13}CH_3$]methionine was performed and showed incorporation rates of 16%–21% into the three methoxy-goups of melithiazol A, which was detected using ^{13}C-NMR spectroscopy (data not shown). Similar results have been obtained in feeding experiments with *Myxococcus fulvus* Mx f333/8, the producer of the methyl ester of myxothiazol A (designated myxothiazol Z) (see Figure 1; [50]).

Heterologous Expression of the Putative Methyltransferase MelK and the Hydrolase MelJ from the Melithiazol Gene Cluster in the Myxothiazol A Producer

M. lichenicola Me I46 proved to be a difficult organism to work with genetically. After severe problems in the generation of the gene library, presumably due to the presence of DNases, the strain showed resistance against almost every antibiotic tested (kanamycin, hygromycin, streptomycin, apramycin, and tetracyclin). Few spontaneously resistant colonies were detected using ampicillin, which encouraged us to try a β-lactamase as marker gene in conjugation and electroporation experiments aimed at the inactivation of *melE*. Because these experiments were not successful, we decided to heterologously express melithiazol biosynthetic genes in *S. aurantiaca* DW4/3-1 to unambigously prove that the right gene cluster was cloned.

MelK and MelJ seemed to be responsible for the formation of the methyl ester. In addition, earlier studies employing *M. fulvus* Mx f333/8 suggested that myxothiazol Z is derived from myxothiazol A via the iminoester intermediate (see Figure 3, [50]). Given the structural analogy between myxothiazol Z and melithiazol A, we speculated that melithiazol A is derived from a melithiazol-amide analogously, which would employ the iminoester of the amide as an intermediate (Figure 3). Nevertheless, the amide could not be identified from *M. lichenicola* Me I46. Alternatively, one could speculate that the methyl ester is formed similarly to the methylation of bacterial chemotaxis transmembrane receptors, e.g., by the protein methyl transferase CheR and the methyl esterase/amidase CheB from *Salmonella typhimurium* [51, 52]. The alternative route would thus involve production of the free myxothiazol acid by MelJ, which then would have to be methylated (Figure 3). MelJ is a protein with all the hallmarks of the nitrilase superfamily of proteins, which includes the amidases. The active site cysteine can be found in position 145 and the catalytic triad glutamate$_{44}$-lysine$_{112}$-cysteine$_{145}$ is responsible for hydrolysis [53]. Both possibilities for methyl ester formation are currently under investigation by heterologous expression and purification of MelJ and MelK. The mechanisms could also be distinguished by feeding $^{13}C/^{18}O$-labeled acetate. If the former is correct, ^{18}O will only be present in the methoxyl oxygen; if the latter is correct, then both the methoxyl and carbonyl oxygens will be labeled so one and two isotope shifts, respectively, should be observed on the carbonyl carbon.

In order to verify the involvement of MelK and MelJ in methyl ester formation, both genes and their presumed promoter region were transferred into the myxothiazol A producer *S. aurantiaca* DW4/3-1 (see Figure 4). For homologous recombination, the DNA region of MtaH was used because this gene is not required for myxothiazol formation (see accompanying manuscript [65]).

Figure 6. Alignment of the MelK Subfamily of SAM-Dependent Methyl Transferases

Kagan and Clarke motifs are indicated by red (motif I), green (post I), yellow (motif II), and blue (motif III) triangles. Black triangles indicate residues binding the SAM cofactor in 1JG4 via side chain atoms, while magenta boxes indicate residues forming the less sequence-specific backbone or hydrophobic contacts to the cofactor in 1JG4. The absolutely conserved Gly in position 110 in 1JG4 is not in direct contact to the cofactor. Amino acid sequences used for the alignment were derived from the following organisms (database entries in brackets): *Mycobacterium leprae* (Q9X7D5), *Homo sapiens* LCMT (see text), *Caenorhabditis elegans* (YKG4_CAEEL), *Streptomyces glaucescens* (TCMP_STRGA), *Pseudomonas aeruginosa* (Q9I2N5), *Rhizobium meliloti* (Q92Y12), *Mycobacterium tuberculosis* (YX99_MYCTU), *Streptomyces coelicolor* (Q9ZBH0), *Actinosynnema pretiosum* ASM10 (see text), *Streptomyces coelicolor* (Q9FBX1), *Anabaena* sp. (Q8YKG6), *Methanosarcina acetivorans* (Q8TLW9), *Methanosarcina mazei* (Q8PWV7), *Mycobacterium tuberculosis* (O33293), *Oceanobacillus iheyensis* (BAC13195), *Bacillus subtilis* (Q45500), *Arabidopsis thaliana* (Q93YR1), *Oryza sativa* (AAN65019), *Rhizobium loti* (Q98LR1), *Pseudomonas aeruginosa* (Q9HX18), *Archaeoglobus fulgibus* (PIM1_ARCFU), *Methanococcus jannaschii* (PIMT_METJA), *Pyrococcus horikoshii* (PIMT_PYRHO), *Aerppyrum pernix* (PIMT_AERPE), and *Pyrococcus furiosus* (Protein Data Base ID code of methyltransferase 1JG4).

After transfer of both genes into the myxothiazol producer, the genotype of the mutant strain was analyzed by Southern hybridizations verifying the correctness of the integration in mutant ESW602 (Figure 4). HPLC-MS analysis of ESW602 culture broth revealed the presence of myxothiazol A and myxothiazol Z (see Figure 5; LC-MS analysis: myxothiazol A, $M + H^+ = 503$; myxothiazol Z, $M + H^+ = 488$), which clearly establishes that MelK and MelJ are responsible for the transformation of the β-methoxyacrylate amide into the β-methoxyacrylate ester.

MelK Is a SAM-Dependent Methyl Transferase with Poorly Conserved SAM Binding Site

Searches for MelK homologs in Swall using Fasta3 [54] gave 41 related proteins, mostly from mycobacteria, streptomyces, and methanosarcina with unknown function, as well as the methyltransferase Asm10 from the *Actinosynnema pretiosum* ansamitocin biosynthetic gene cluster [55]. Asm10 is the only biochemically characterized member of this group of proteins. The recombinant enzyme catalyzes the final step in ansamitocin biosynthesis, the SAM-dependent N-methylation of the amide linkage (G. Shang, P. Spiteller, L. Bai, B.J. Carroll, T.-W. Yu, and H.G. Floss, personal communication). No significant similarities to structurally known SAM-dependent methyl transferases specific either for small molecule, protein, DNA, or RNA were detected initially. For these, it has been demonstrated that they share only little sequence identity but contain a highly conserved structural fold with the poorly conserved SAM binding residues [56]. In contrast to the O-MT domains of MelE and MelF, which match the formerly proposed core sequences perfectly (see Supplemental Figure S1 at *Chemistry & Biology*'s website; [46]), these signature sequences are difficult to identify in MelK and the related sequences. A brain protein phosphatase 2A leucine carboxyl methyltransferase (LCMT) uses SAM as cofactor. It harbors four regions that coincide fairly well with the Kagan and Clarke binding motifs I–III and the additional post I motif [57]. However, a profile fitting alignment of the MelK-related sequences with the protein-L-isoaspartate O-methyltransferase from *Pyrococcus furiosus* (Protein Data Bank ID code 1JG4) and other sequences from the Pimt branch of SAM-dependent methyltransferases (EC 2.1.1.77) shows reasonable similarity of the motifs identified by Kagan and Clarke in the MelK-related sequences, making it plausible to include these enzymes in the large family of SAM-dependent methyltransferases. Figure 6 shows an alignment of MelK and related proteins from diverse organisms together with some typical Pimt methyltransferases. The Kagan and Clarke motifs are indicated by red (motif I), green (post I), yellow (motif II), and blue (motif III) triangles. Black triangles indicate residues binding the SAM cofactor in 1JG4 via side chain atoms, which are therefore sequence specific, while magenta boxes indicate residues forming less sequence specific backbone or hydrophobic contacts to the cofactor in 1JG4. Two of the four residues forming side chain contacts to the cofactor in 1JG4 display conservative amino acid substitutions (Gly/Ala 108 and Glu/Asp 128); all other residues are not conserved, which has already been observed by Martin and McMillan as common to the methyltransferases. The absolutely conserved Gly in position 110 in 1JG4 is not in direct contact with the cofactor, but on one side of the binding pocket. It is located in a position where any amino acid side chain would interfere with the cofactor sulfur atom. Thus, it can be expected that MelK, as Asm10 and LCMT, binds the SAM-cofactor similarly to the other methyltransferases and contains the typical SAM binding fold.

Evolutionary Aspects of Melithiazol and Myxothiazol Biosynthesis

It is interesting to note that the myxothiazol gene cluster must have evolved from the melithiazol gene cluster or vice versa, which can be shown by sequence comparison (Figure 2); MelC-H and MtaC-H are highly homologous (the encoding genes are very similar in sequence as well; see Figure 2) and are presumed to have similar functions in melithiazol and myxothiazol biosynthesis. Even the large identical repeat within the AT of *mtaD* and *mtaF* (1223 bp, 99.7% identity) is found in *melD* and *melF* as well (1222 bp, 99.1% identity). Unexpectedly, when the *mel* and *mta* repeat regions are compared, they are not identical and do not show higher similarities with each other than the complete genes. MtaB and MelB are involved in the formation of the PKS starter molecule, which is different in both biosyntheses. Accordingly, the corresponding genes show lower similarity scores. Nevertheless, the KS-AT-ACP fragment of the second module of MtaB clearly resembles MelB. All the other KS, AT, and ACP domains of the myxothiazol gene cluster are much less similar to those of MelB (Figure 2). This suggests that MelB evolved from MtaB by deletion of the reductive loop of the second module of MtaB accompanied by the additional loss of the loading module and the first module of MtaB. Alternatively, domain and module insertions might have caused the generation of MtaB from MelB. Unexpectedly, no similarities were found in the sequences flanking the PKS/NRPS regions. No similar genes to *mtaA* and ORFA are located upstream and downstream of the *mel* region in *M. lichenicola* Me l46.

Significance

Myxobacteria are a rich source of secondary metabolites with biological activity. In contrast to actinomycetes, molecular analyses of biosynthetic systems are rare, and genetic systems are still lacking for most myxobacterial genera. Nevertheless, a considerable variety of hybrid PKS/NRPS compounds from myxobacteria makes the corresponding biosynthetic machineries very interesting targets to study. The melithiazol PKS/NRPS hybrid described in this publication has been analyzed because of the effectiveness of the compound as inhibitor of the eukaryotic respiratory chain. In addition, the availability of the gene cluster allows the comparison with the myxothiazol system, which is similar but shows significant biosynthetic differences. Considerable information can be gained about unusual domains in PKS and NRPS, e.g., O-methyl

transferase domains embedded in PKS and oxidase and monooxygenase domains embedded in NRPS. The formation of the terminal amide of myxothiazol is clearly NRPS dependent, and glycine has been established as the nitrogen source. This is presumably a general mechanism for amide formation in bacteria. Unexpectedly, the mechanism of methyl-ester formation in melithiazol biosynthesis involves the amide intermediate as well. Heterologous expression of MelK and MelJ results in the formation of the methyl ester of myxothiazol. MelK belongs to a new subclass of SAM-dependent methyl transferases with low homology to the typical SAM binding motif. Most proteins of the same subclass have a unknown function and might be involved in regulation processes, e.g., via protein methylation.

Experimental Procedures

Bacterial Strains and Culture Conditions

Escherichia coli and *S. aurantiaca* DW4/3-1 and its descendants were cultured as described previously [12, 58]. *M. lichenicola* Me I46 was cultivated in M7 liquid medium containing probion ME 0.5%, $CaCl_2 \times 2\ H_2O$ 0.1%, $MgSO_4 \times 7\ H_2O$ 0.1%, yeast extract 0.1%, soluble starch 0.5%, and HEPES buffer 50 mM (pH 7.2). One hundred milliliter cultures in 250 ml Erlenmeyer flasks were incubated at 30°C on a gyratory shaker at 160 rpm for 4–5 days.

DNA Manipulations, Analysis, Sequencing, and PCR

Chromosomal DNA from *S. aurantiaca* DW4/3-1 and *M. lichenicola* Me I46 was prepared as described [59]. Southern Blot analysis of genomic DNA was performed using the standard protocol for homologous probes of the DIG DNA labeling and detection kit (Roche Diagnostics, Mannheim, Germany).

Sequencing of cosmids M1 and M2 was performed by a shotgun approach: sheared fragments of the two cosmids were subcloned separately into pTZ18R. About 500 clones were selected from each cosmid library, and plasmid DNA was prepared (Millipore) and sequenced using DYEnamic ET terminator cycle sequencing premix kit (Amersham Pharmacia Biotech) and UPO/PRO primers (MWG-Biotech). The gels were run on ABI-377 sequencers, and data were assembled and edited using the XGAP program [60].

PCR was carried out using *Pfu*-DNA-Polymerase (Stratagene) according to the manufacturer's protocol with the addition of 5% DMSO. Conditions for amplification with the Eppendorf Mastercycler gradient (Eppendorf, Germany) were as follows: denaturation for 30 s at 95°C, annealing for 30 s at 60°C, and extension for 45 s at 72°C, 30 cycles and a final extension at 72°C for 10 min. Primers used for the amplification of internal fragments of *mtaH* were E3, 5′-TCG GCA GGA AGA AGT CGT C-3 and E4, 5′-CTC GGG ATC CAG CAG GTA G-3′.

All other DNA manipulations were performed according to standard protocols [61]. Amino acid and DNA alignments were done using the programs of the Lasergene software package (DNAstar Inc.) and ClustalW [62].

Colony Hybridization

Colony Hybridization was carried out according to the manufacturer's protocol (Roche Diagnostics, Mannheim) under stringent conditions. Screening probes were derived from *mtaE* and *mtaF* (oligonucleotides METE1FOR 5′-CAG AGC TCG AGG TCA TGT TGC AGT CGC-3′ and METE4REV 5′-GCT CTA GAT GAG CCC GAA GCG CTT GGA C-3′ were used to generate the probe derived from *mtaE*, and primer pair SW1 5′-AGG TGG GGC CGA AGC CGA CGT TG-3′ + SW4 5′-GGA TGC CGT GCA GGT GCT TCT-3 was used to generate the probe derived from *mtaF*). Cosmid M1 hybridized with both probes.

Preparation and Screening of the Cosmid Library

The cosmid gene library of *M. lichenicola* Me I46 was made as described for *S. aurantiaca* Sg a15 [63]. Approximately 1900 cosmid-harboring single colonies were picked into 96-well microtiter plates, grown in LB medium overnight, and replicated twice. Twenty-five percent glycerol was added to one copy of the library, and the plates were frozen at −80°C. The colonies of the second copy were transferred onto a nylon membrane (Biodyne B, Pall), which was used for the colony hybridization. Cell mass of 16 clones of each plate of the third copy was collected, and cosmid DNA from each "pool" was prepared. These "cosmid pools" were used as templates in PCR reactions with primer pair MEL1, 5′-ATC CGG GTC TTC GCG CGC GAC A-3′ and MEL3L, 5′-GGA TCC TCC AGG AAG AGC GAG G-3′, which were designed to specifically bind to the insert located at the T7 end of cosmid M1. DNA of single cosmids from the pools giving a PCR product of the expected size (350 bp) were used as templates in a second round of PCR. Positive clones were further analyzed by Southern blot hybridization using probes derived from the *mta* gene cluster. Additionally, these cosmids were end sequenced, and the derived sequences were compared with the sequence of the *mta* gene cluster.

Production and Analysis of Secondary Metabolites in *S. aurantiaca* DW4/3-1 and Its Descendants

The cultivation of the strains, the preparation of the culture extracts, and the conditions for the analysis of the spectrum of secondary metabolites using diode array-coupled HPLC were desribed previously [12]. A solvent gradient was applied using 0.2% aqueous acetic acid (solvent A) and acetonitrile (solvent B): 50% B at 0 min to 70% B at 15 min. Subsequently, the percentage of solvent B was increased in a gradient up to 100% within 1 min. The flow rate was 0.5 ml/min while detection was carried out at 254 nm.

Heterologous Expression of *melJ* and *melK*

Hydrolysis of cosmid M1 with StuI yields four DNA fragments with sizes between 3.1 and 3.2 kb. The target fragment harbors at its 5′ end a 309 bp deletion of *melH* and the complete genes *melJ* and *melK*. Additional 670 bp in front of *melK* presumably harbor the promoter region regulating the transcription of *melJK* (Figure 4). For heterologous expression of *melJ* and *melK* in *S. aurantiaca* DW4/3-1, the mixture of four fragments was subcloned into pCR-XL-TOPO (Invitrogen) after restriction of cosmid M1 and extension of the fragments using *Taq*-DNA-polymerase. Clones were analyzed by restriction and sequencing, resulting in the identification of plasmid pMSW12 harboring the 3264 bp target fragment. To allow homologous recombination in *S. aurantiaca* DW4/3-1 via *mtaH*, the insert of pESW26 (532 bp PCR-product generated using primers E3 and E4 from cosmid E201 [12] and cloned into pCR-2.1-TOPO) was isolated after digestion with NotI/SpeI and cloned into NotI/XbaI predigested pMSW12, which resulted in pESW243. This plasmid was transferred into the chromosome of *S. aurantiaca* DW4/3-1 by homologous recombination as described previously [12], and the mutants were analyzed as described in the accompanying manuscript [65].

Feeding Experiments Employing Labeled Precursors

[$^{13}CH_3$]Methionine

One liter of M7 medium in 2 l Erlenmeyer flasks was inoculated with 50 ml of 3-day-old *M. lichenicola* Me I46 culture and grown at 30°C (170 rpm in a gyratory shaker). Ten milligrams of [$^{13}CH_3$]methionine (Campro Scientific) was dissolved in 10 ml water and sterilized using a membrane filter. The compound was pulse fed as follows: 6 mg after 24 hr, 2 mg each after 48 and 72 hr. One percent (v/v) XAD-adsorber resin (Rohm & Haas) was added after 72 hr. After incubating for 96 hr, cells and resin were harvested by centrifugation, and the pellet was extracted and analyzed as described by ^{13}C-NMR [26]. Incorporation rates were calculated by comparison to an internal standard.

d8-DL-Valine

Fifty milliliters of M7 medium in 250 ml Erlenmeyer flasks was inoculated with 2 ml of a culture of *M. lichenicola* Me I46 (3 days old) and grown at 30°C (170 rpm in a gyratory shaker). Fifteen milligrams of deuterated d8-DL-Valine (Cambridge Isotope Laboratories) was added at 24 hr, 48 hr, and 72 hr. After 72 hr, XAD-adsorber resin was added (1% [v/v]), and cells were grown for another 24 hr. Subsequently, cells and resin were harvested by centrifugation and ex-

tracted twice (first using 30 ml methanol and then with 20 ml acetone). Combined extracts were dried under vacuo and redissolved in 500 μl methanol. The analysis was performed after injection of 5 μl of the extract into a HPLC-MS Agilent 1100 LC system. The following solvents were used: A, 5% acetonitrile, 95% water, 5 mM ammonium acetate (NH_4Ac), 0.003% acetic acid; B, 95% acetonitrile, 5% water, 5 nM NH_4Ac, 0.003% acetic acid. A solvent gradient was applied as follows: 10% B at 0 min to 100% B within 30 min, then 10 min with 100% B. The flow rate was 0.3 ml/min and the UV detection was carried out at 220 nm. For mass detection, a PE Sciex API 2000 mass spectrometer equipped with a TurbolonSpray source was used.

^{15}N-Glycine, ^{15}N-Glutamate, and ^{15}N-Ammonium Chloride

S. aurantiaca DW 4/3-1 was inoculated in 20 ml tryptone-starch medium [41] and cultivated at 28°C (200 rpm in a gyratory shaker) for 2 days. Ten milliliters of the culture was then transferred to a 500 ml erlenmeyer flask containing 200 ml tryptone-starch medium, and the flask was shaken at 30°C (160 rpm). Thirty milligrams of each of the labeled precursors (^{15}N-Glycine, ^{15}N-glutamate, and ^{15}N-ammonium chloride) was dissolved in 2 ml water and sterilized through a 0.22 μm diameter pore size ultrafilter (Millipore, Millex-GV4). The labeled precursors were pulse fed in two equal portions 24 and 48 hr after inoculation. Cells were harvested after 4 days of cultivation, and the products were extracted with acetone. Myxothiazol was purified by silica gel column chromatography (n-hex:EtOAc 5:1 ∼ n-hex-EtOAc 1:1, EtOAc) and subsequently by HPLC (YMC-Pack ODS-AQ, 250 ×10 mm, methanol:water 82:18). The incorporation rate of ^{15}N into myxothiazol was determined using single ion monitoring in a electrospray mass spectrometer [64].

Acknowledgments

The authors would like to thank Prof. Dr. H. Reichenbach for strain *M. lichenicola* Me I46. We are grateful to Prof. Dr. G. Höfle and Dr. B. Kunze for help with the analysis of myxothiazol and its derivatives and to M. Scharfe and Dr. H. Blöcker for their support concerning the sequencing of cosmid M2. B.R.T. Higa contributed to the analysis of the ^{15}N-feeding studies. Work in R.M.'s laboratory was supported by the Deutsche Forschungsgemeinschaft (grants Mu1254/3-3 and Mu1254/6-1). We acknowledge the generous gift of ^{15}N-labeled substances and the helpful comments by B. Carroll and Prof. Dr. H.G. Floss regarding this manuscript.

Received: April 7, 2003
Revised: July 31, 2003
Accepted: August 6, 2003
Published: October 17, 2003

References

1. Cane, D.E. (1997). Polyketide and nonribosomal polypeptide biosynthesis. Chem. Rev. *97*, 2463–2464.
2. Staunton, J., and Weissman, K.J. (2001). Polyketide biosynthesis: a millennium review. Nat. Prod. Rep. *18*, 380–416.
3. Konz, D., and Marahiel, M.A. (1999). How do peptide synthetases generate structural diversity? Chem. Biol. *6*, R39–R48.
4. Lambalot, R.H., Gehring, A.M., Flugel, R.S., Zuber, P., LaCelle, M., Marahiel, M.A., Reid, R., Khosla, C., and Walsh, C.T. (1996). A new enzyme superfamily–the phosphopantetheinyl transferases. Chem. Biol. *3*, 923–936.
5. Molnar, I., Aparicio, J.F., Haydock, S.F., Khaw, L.E., Schwecke, T., Konig, A., Staunton, J., and Leadlay, P.F. (1996). Organisation of the biosynthetic gene cluster for rapamycin in *Streptomyces hygroscopicus*: analysis of genes flanking the polyketide synthase. Gene *169*, 1–7.
6. August, P.R., Tang, L., Yoon, Y.J., Ning, S., Müller, R., Yu, T.W., Taylor, M., Hoffmann, D., Kim, C.G., Zhang, X., et al. (1998). Biosynthesis of the ansamycin antibiotic rifamycin: deductions from the molecular analysis of the rif biosynthetic gene cluster of *Amycolatopsis mediterranei* S699. Chem. Biol. *5*, 69–79.
7. Gehring, A.M., DeMoll, E., Fetherston, J.D., Mori, I., Mayhew, G.F., Blattner, F.R., Walsh, C.T., and Perry, R.D. (1998). Iron acquisition in plague: modular logic in enzymatic biogenesis of yersiniabactin by *Yersinia pestis*. Chem. Biol. *5*, 573–586.
8. O'Connor, S.E., Chen, H.W., and Walsh, C.T. (2002). Enzymatic assembly of epothilones: The EpoC subunit and reconstitution of the EpoA-ACP/B/C polyketide and nonribosomal peptide interfaces. Biochemistry *41*, 5685–5694.
9. Admiraal, S.J., Khosla, C., and Walsh, C.T. (2002). The loading and initial elongation modules of rifamycin synthetase collaborate to produce mixed aryl ketide products-1. Biochemistry *41*, 5313–5324.
10. Cane, D., and Walsh, C. (1999). The parallel and convergent universes of polyketide synthases and nonribosomal peptide synthetases. Chem. Biol. *6*, R319–R325.
11. Reichenbach, H., and Höfle, G. (1999). Myxobacteria as producers of secondary metabolites. In Drug Discovery from Nature, S. Grabley and R. Thieriecke, eds. (Berlin: Springer Verlag), pp. 149–179.
12. Silakowski, B., Schairer, H.U., Ehret, H., Kunze, B., Weinig, S., Nordsiek, G., Brandt, P., Blöcker, H., Höfle, G., Beyer, S., et al. (1999). New lessons for combinatorial biosynthesis from myxobacteria: the myxothiazol biosynthetic gene cluster of *Stigmatella aurantiaca* DW4/3–1. J. Biol. Chem. *274*, 37391–37399.
13. Paitan, Y., Alon, G., Orr, E., Ron, E.Z., and Rosenberg, E. (1999). The first gene in the biosynthesis of the polyketide antibiotic TA of *Myxococcus xanthus* codes for a unique PKS module coupled to a peptide synthetase. J. Mol. Biol. *286*, 465–474.
14. Molnar, I., Schupp, T., Ono, M., Zirkle, R.E., Milnamow, M., Nowak-Thompson, B., Engel, N., Toupet, C., Stratman, A., Cyr, D.D., et al. (2000). The biosynthetic gene cluster for the microtubule-stabilizing agents epothilones A and B from *Sorangium cellulosum* So ce90. Chem. Biol. *7*, 97–109.
15. Julien, B., Shah, S., Ziermann, R., Goldman, R., Katz, L., and Khosla, C. (2000). Isolation and characterization of the epothilone biosynthetic gene cluster from *Sorangium cellulosum*. Gene *249*, 153–160.
16. Silakowski, B., Kunze, B., Nordsiek, G., Blöcker, H., Höfle, G., and Müller, R. (2000). The myxochelin iron transport regulon of the myxobacterium *Stigmatella aurantiaca* Sg a15. Eur. J. Biochem. *267*, 6476–6485.
17. Gaitatzis, N., Kunze, B., and Müller, R. (2001). *In vitro* reconstitution of the myxochelin biosynthetic machinery of *Stigmatella aurantiaca* Sg a15: Biochemical characterization of a reductive release mechanism from nonribosomal peptide synthetases. Proc. Natl. Acad. Sci. USA *98*, 11136–11141.
18. Gaitatzis, N., Silakowski, B., Kunze, B., Nordsiek, G., Blöcker, H., Höfle, G., and Müller, R. (2002). The biosynthesis of the aromatic myxobacterial electron transport inhibitor stigmatellin is directed by a novel type of modular polyketide synthase. J. Biol. Chem. *277*, 13082–13090.
19. Silakowski, B., Nordsiek, G., Kunze, B., Blöcker, H., and Müller, R. (2001). Novel features in a combined polyketide synthase/non-ribosomal peptide synthetase: The myxalamid biosynthetic gene cluster of the myxobacterium *Stigmatella aurantiaca* Sg a15. Chem. Biol. *8*, 59–69.
20. Nishizawa, T., Ueda, A., Asayama, M., Fujii, K., Harada, K., Ochi, K., and Shirai, M. (2000). Polyketide synthase gene coupled to the peptide synthetase module involved in the biosynthesis of the cyclic heptapeptide microcystin. J. Biochem. (Tokyo) *127*, 779–789.
21. Tillett, D., Dittmann, E., Erhard, M., von Döhren, H., Börner, T., and Neilan, B.A. (2000). Structural organization of microcystin biosynthesis in *Microcystis aeruginosa* PCC7806: an integrated peptide-polyketide synthetase system. Chem. Biol. *7*, 753–764.
22. Chang, Z.X., Flatt, P., Gerwick, W.H., Nguyen, V.A., Willis, C.L., and Sherman, D.H. (2002). The barbamide biosynthetic gene cluster: a novel marine cyanobacterial system of mixed polyketide synthase (PKS)-non-ribosomal peptide synthetase (NRPS) origin involving an unusual trichloroleucyl starter unit. Gene *296*, 235–247.

23. Gerth, K., Irschik, H., Reichenbach, H., and Trowitzsch, W. (1980). Myxothiazol, an antibiotic from *Myxococcus fulvus* (myxobacterales). I. Cultivation, isolation, physico-chemical and biological properties. J. Antibiot. *33*, 1474–1479.
24. Trowitzsch, W., Reifenstahl, G., Wray, V., and Höfle, G. (1980). Myxothiazol, an antibiotic from *Myxococcus fulfus* (Myxobacteraoles) II. Structure elucidation. J. Antibiot. *33*, 1480–1490.
25. Sasse, F., Böhlendorf, B., Hermann, M., Kunze, B., Forche, E., Steinmetz, H., Höfle, G., and Reichenbach, H. (1999). Melithiazols, new β-methoxyacrylate inhibitors of the respiratory chain isolated from myxobacteria–production, isolation, physicochemical and biological Properties. J. Antibiot. *52*, 721–729.
26. Böhlendorf, B., Herrmann, M., Hecht, H.J., Sasse, F., Forche, E., Kunze, B., Reichenbach, H., and Höfle, G. (1999). Antibiotics from gliding bacteria—melithiazols A-N: new antifungal β-methoxyacrylates from myxobacteria. Eur. J. Org. Chem. *10*, 2601–2608.
27. Gaitatzis, N., Hans, A., Müller, R., and Beyer, S. (2001). The *mtaA* gene of the myxothiazol biosynthetic gene cluster from *Stigmatella aurantiaca* DW4/3–1 encodes a phosphopantetheinyl transferase that activates polyketide synthases and polypeptide synthetases. J. Biochem. *129*, 119–124.
28. Silakowski, B., Kunze, B., and Müller, R. (2001). Multiple hybrid polyketide synthase/non-ribosomal peptide synthetase gene clusters in the myxobacterium *Stigmatella aurantiaca*. Gene *275*, 233–240.
29. Gehring, A.M., DeMoll, E., Fetherston, J.D., Mori, I., Mayhew, G.F., Blattner, F.R., Walsh, C.T., and Perry, R.D. (1998). Iron acquisition in plague: modular logic in enzymatic biogenesis of yersiniabactin by *Yersinia pestis*. Chem. Biol. *5*, 573–586.
30. Kennedy, J., Auclair, K., Kendrew, S.G., Park, C., Vederas, J.C., and Hutchinson, C.R. (1999). Modulation of polyketide synthase activity by accessory proteins during lovastatin biosynthesis. Science *284*, 1368–1372.
31. Chen, H.W., O'Connor, S., Cane, D.E., and Walsh, C.T. (2001). Epothilone biosynthesis: assembly of the methylthiazolylcarboxy starter unit on the EpoB subunit. Chem. Biol. *8*, 899–912.
32. Walsh, C.T., Chen, H.W., Keating, T.A., Hubbard, B.K., Losey, H.C., Luo, L.S., Marshall, C.G., Miller, D.A., and Patel, H.M. (2001). Tailoring enzymes that modify nonribosomal peptides during and after chain elongation on NRPS assembly lines. Curr. Opin. Chem. Biol. *5*, 525–534.
33. Donadio, S., Staver, M.J., McAlpine, J.B., Swanson, S.J., and Katz, L. (1991). Modular organization of genes required for complex polyketide biosynthesis. Science *252*, 675–679.
34. Schwecke, T., Aparicio, J.F., Molnar, I., König, A., Khaw, L.E., Haydock, S.F., Oliynyke, M., Caffrey, P., Cortes, J., Lester, J.B., et al. (1995). The biosynthetic gene cluster for the polyketide immunosuppressant rapamycin. Proc. Natl. Acad. Sci. USA *92*, 7839–7843.
35. Kleinkauf, H., and von Döhren, H. (1997). Products of secondary metabolism. In Biotechnology, H. Kleinkauf and H. von Döhren, eds. (Weinheim, Germany: Verlag Chemie), pp. 277–322.
36. Shimkets, L. (1993). The myxobacterial genome. In Myxobacteria II, M. Dworkin and D. Kaiser, eds. (Washington, D.C.: American Society for Microbiology), pp. 85–108.
37. Bisang, C., Long, P., Cortes, J., Westcott, J., Crosby, J., Matharu, A.-L., Cox, R., Simpson, T., Staunton, J., and Leadlay, P. (1999). A chain initiation factor common to both modular and aromatic polyketide synthases. Nature *401*, 502–505.
38. Ligon, J., Hill, S., Beck, J., Zirkle, R., Molnar, I., Zawodny, J., Money, S., and Schupp, T. (2002). Characterization of the biosynthetic gene cluster for the antifungal polyketide soraphen A from *Sorangium cellulosum* So ce26. Gene *285*, 257–267.
39. Wilkinson, C.J., Frost, E.J., Staunton, J., and Leadlay, P.F. (2001). Chain initiation on the soraphen-producing modular polyketide synthase from *Sorangium cellulosum*. Chem. Biol. *8*, 1197–1208.
40. Trowitzsch-Kienast, W., Wray, V., Gerth, K., Reichenbach, H., and Höfle, G. (1986). Antibiotika aus Gleitenden Bakterien, XXVIII: Biosynthese des Myxothiazols in *Myxococcus fulvus* Mx f16. Liebigs Ann. Chem. *10*, 93–98.
41. Mahmud, T., Bode, H.B., Silakowski, B., Kroppenstedt, R.M., Xu, M., Nordhoff, S., Höfle, G., and Müller, R. (2002). A novel biosynthetic pathway providing precursors for fatty acid biosynthesis and secondary metabolite formation in myxobacteria. J. Biol. Chem. *277*, 32768–32774.
42. Long, P.F., Wilkinson, C.J., Bisang, C.P., Cortes, J., Dunster, N., Oliynyk, M., McCormick, E., McArthur, H., Mendez, C., Salas, J.A., et al. (2002). Engineering specificity of starter unit selection by the erythromycin-producing polyketide synthase. Mol. Microbiol. *43*, 1215–1225.
43. Challis, G., Ravel, J., and Townsend, C. (2000). Predictive, structure-based model of amino acid recognition by nonribosomal peptide synthetase adenylation domains. Chem. Biol. *7*, 211–224.
44. Stachelhaus, T., Mootz, H.D., and Marahiel, M.A. (1999). The specificity-conferring code of adenylation domains in nonribosomal peptide synthetases. Chem. Biol. *6*, 493–505.
45. Smith, S. (1994). The animal fatty acid synthase: one gene, one polypeptide, seven enzymes. FASEB J. *8*, 1248–1259.
46. Kagan, R.M., and Clarke, S. (1994). Widespread occurrence of three sequence motifs in diverse S-adenosylmethionine-dependent methyltransferases suggest a common structure for these enzymes. Arch. Biochem. Biophys. *310*, 417–427.
47. Kulathila, R., Merkler, K.A., and Merkler, D.J. (1999). Enzymatic formation of C-terminal amides. Nat. Prod. Rep. *16*, 145–154.
48. Schoof, L., Veelaert, D., Vanden Broeck, J., and De Loof, A. (1997). Peptides in the locusts, *Locusta migratoria* and *Schistocerca gregaria*. Peptides *18*, 145–156.
49. Mocek, U., Knaggs, A.R., Tsuchiya, R., Nguyen, T., Beale, J.M., and Floss, H.G. (1993). Biosynthesis of the modified peptide antibiotic nosiheptide in *Streptomyces actuosus*. J. Am. Chem. Soc. *115*, 7557–7568.
50. Steinmetz, H., Forche, E., Reichenbach, H., and Höfle, G. (2000). Biosynthesis of myxothiazol Z, the ester-analog of myxothiazol A in *Myxococcus fulvus*. Tetrahedron *56*, 1681–1684.
51. Djordjevic, S., and Stock, A. (1997). Crystal structure of the chemotaxis receptor methyltransferase CheR suggests a conserved structural motif for binding S-adenosylmethionine. Curr. Biol. *5*, 545–558.
52. Koshland, D., Jr. (1988). Chemotaxis as a model second-messenger system. Biochemistry *27*, 5829–5833.
53. Pace, H., and Brenner, C. (2001). The nitrilase superfamily: classification, structure and function. Genome Biol. *2*, 0001.0001–0001.0008.
54. Pearson, W.R., and Lipman, D.J. (1988). Improved tools for biological sequence comparison. Proc. Natl. Acad. Sci. USA *85*, 2444–2448.
55. Yu, T.-W., Bai, L., Clade, D., Hoffmann, D., Toelzer, S., Trinh, K.Q., Xu, J., Moss, S.J., Leistner, E., and Floss, H.G. (2002). The biosynthetic gene cluster of the maytansinoid antitumor agent ansamitocin from *Actinosynnema pretiosum*. Proc. Natl. Acad. Sci. USA *99*, 7968–7973.
56. Martin, J., and McMillan, F. (2002). SAM (dependent) I AM: the S-adenosylmethionine-dependent methyltansferase fold. Curr. Opin. Struct. Biol. *12*, 783–793.
57. De Baere, I., Derua, R., Janssens, V., Van Hoof, C., Waelkens, E., Merlevede, W., and Goris, J. (1999). Purification of porcine brain protein phosphatase 2A leucine carboxyl methyltransferase and cloning of the human homologue. Biochemistry *38*, 16539–16547.
58. Silakowski, B., Ehret, H., and Schairer, H.U. (1998). *fbfB*, a gene encoding a putative galactose oxidase, is involved in *Stigmatella aurantiaca* fruiting body formation. J. Bacteriol. *180*, 1241–1247.
59. Neumann, B., Pospiech, A., and Schairer, H.U. (1992). Rapid isolation of genomic DNA from Gram negative bacteria. Trends Genet. *8*, 332–333.
60. Bonfield, J., Smith, K., and Staden, R. (1995). Nucleic Acids Res *23*, 4992–4999.
61. Sambrook, J., Fritsch, E.F., and Maniatis, T. eds. (1989). Molecular Cloning: A Laboratory Manual, Second Edition (Cold Spring Harbor, NY: Cold Spring Harbor Laboratory Press).

62. Thompson, J.D., Higgins, D.G., and Gibson, T.J. (1994). CLUSTAL W: Improving the sensitivity of progressive multiple sequence alignment through sequence weighting, position-specific gap penalties and weight matrix choice. Nucleic Acids Res. *22*, 4673–4680.
63. Beyer, S., Kunze, B., Silakowski, B., and Müller, R. (1999). Metabolic diversity in myxobacteria - identification of the myxalamid and the stigmatellin biosynthetic gene cluster of *Stigmatella aurantiaca* Sg a15 and a combined polyketide- (poly)peptide gene cluster from the epothilon producing strain *Sorangium cellulosum* So ce90. Biochim. Biophys. Acta *1445*, 185–195.
64. Morgan, J., Joyce-Menekse, M., Rowlands, R., Gilbert, I., and Lloyd, D. (2001). Rapid and sensitive quantitation of antibiotics in fermentations by electrospray mass spectrometry. Rapid Commun. Mass Spectrom. *15*, 1229–1238.
65. Weinig, S., Mahmud, T., and Müller, R. (2003). Markerless mutations in the myxothiazol biosynthetic gene cluster: a delicate megasynthetase with a superfluous nonribosomal peptide synthetase domain. Chem. Biol. *10*, this issue, 953–960.

Accession Numbers

The nucleotide sequence reported here has been submitted to the EMBL database under accession number AJ557546.